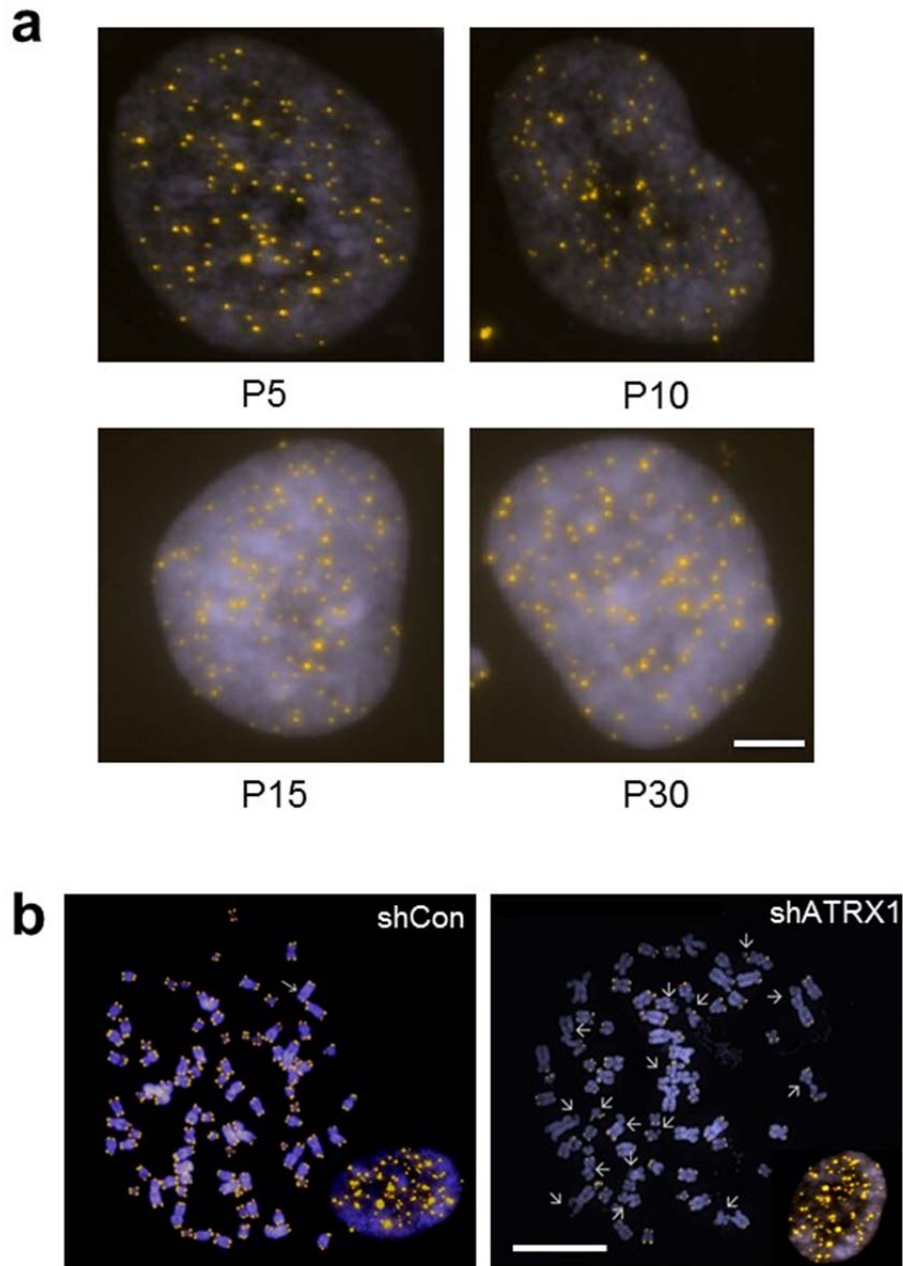


741

742

743 **Supplementary FIG. 1: ATRX deficiency promotes G4 formation.** **a:** G4 staining in
744 primary murine neural progenitor cells harboring either intact or inactivated *Atrx*³⁸. **b:**
745 NHAs treated with 50nM CX-3543 alone (left), or with either DNase (middle), or RNase
746 (right) to confirm the specificity of the 1H6 antibody. **c:** Confirmation of specificity for Hf2
747 G4 pulldowns using kit2 G4 nucleotides. Hf2 antibodies were incubated with
748 kit2+random ssDNA mixture, no elution (lane 4), kit2+random dsDNA, no elution (lane
749 5), ssDNA alone (lane 6), dsDNA alone (lane 7), kit2+ssDNA, eluted (lane 8) and
750 kit2+dsDNA, eluted (lane 9). Kit2 (lane 1), ssDNA (lane 2) and dsDNA (lane 3) were also
751 included in the electrophoresis. Samples were run on a 3% agarose gel, non-denaturing.
752 Arrows showed gel shift due to binding of pulldown antibodies. **d-f:** Inducible NHA lines
753 showed no effects of ATRX inactivation on either apoptosis (measured by Annexin V
754 positive population, d) or proliferation (measured by BrdU incorporation, e; G2/M-phase
755 content (4n), f).
756



757

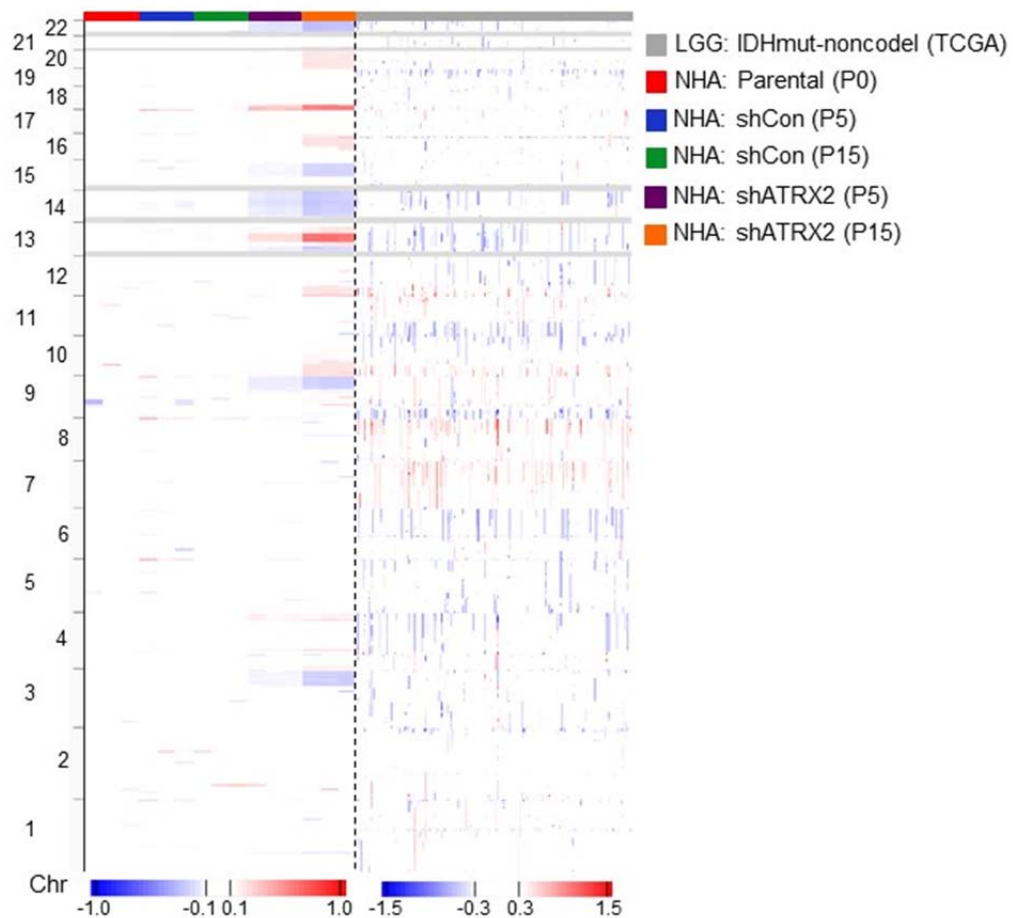
758 **Supplementary FIG. 2: ATRX knockdown induces chromosome breaks, but not**

759 **ALT in NHAs. a:** TEL-FISH of NHAs at passages 5, 10, 15 and 30 after ATRX

760 knockdown. **b:** ATRX deficient NHAs (shATRX1, passage 15) showed significantly

761 increased chromosome breaks by cytogenetic analysis. Despite these chromosome

762 abnormalities, Tel-FISH (yellow) showed no change in telomere signal.



763
764

Supplementary FIG. 3: ATRX deficiency induces CNAs in NHAs and is associated

765

with a distinct CNA profile in gliomas. Segmented SNP array data for parental NHAs,

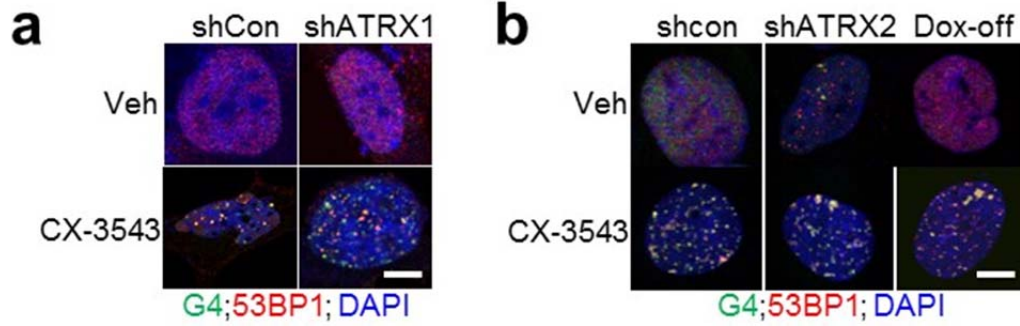
766

shCon NHAs (P5 and P15), shATRX1 NHAs (P5 and p15) and IDHmut-noncodel LGG

767

patients visualized by IGV.

768



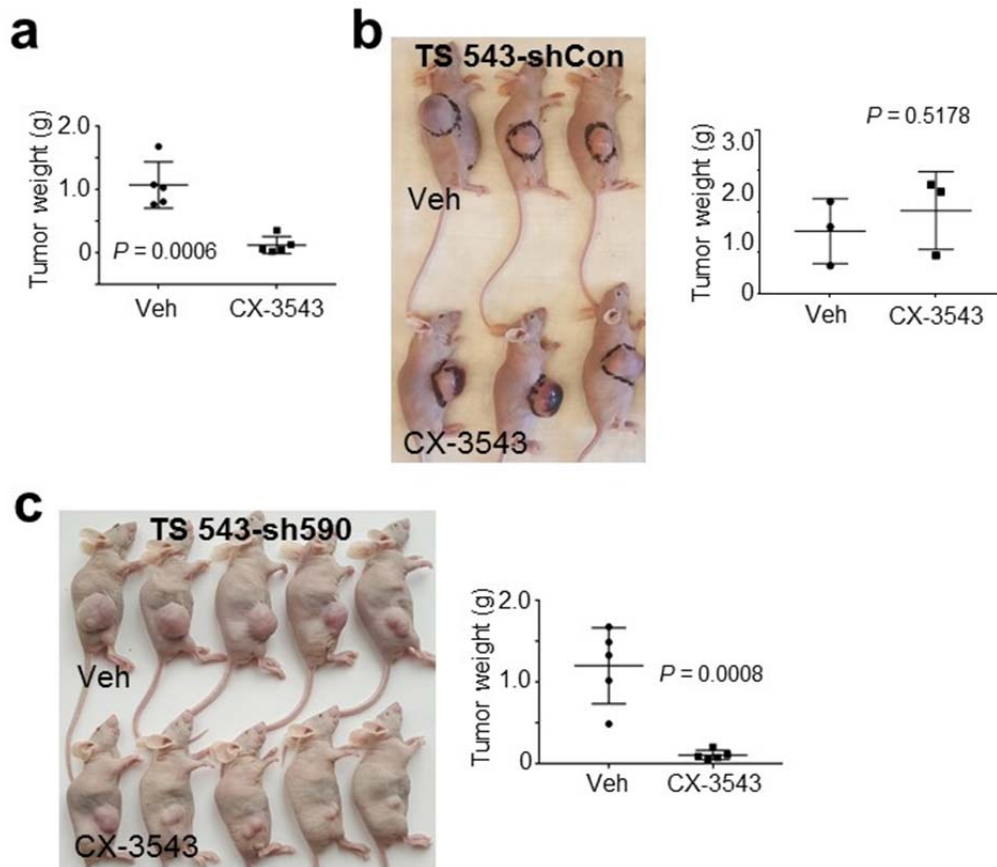
769
 770

Supplementary FIG. 4: G4s colocalize with DNA damage foci induced by CX-3543.

771 G4 and 53BP1 coimmunofluorescence of stable (a) and inducible (b) shATRX NHAs

772 treated with 100 nM CX-3543 (DAPI counterstain).

773



774

775 **Supplementary FIG. 5: CX-3543 markedly slows the growth of ATRX-mutant**
 776 **glioma xenografts *in vivo*.** **a:** Tumor weights of JHH-273 xenografts at study endpoint
 777 (See Materials and Methods) following treatment with either vehicle control (Veh) or 12.5
 778 mg/kg CX-3543. **b:** Representative image of mice bearing TS 543 (ATRX intact)
 779 xenografts following treatment with either vehicle (veh) or 12.5 mg/kg CX-3543 for 24
 780 days. Tumor weights of TS543-shCon xenografts at study endpoint (See Materials and
 781 Methods) following treatment with either vehicle control (Veh) or 12.5 mg/kg CX-3543
 782 are also shown. **c:** Representative image of mice bearing TS 543 (sh590-ATRX
 783 knockdown) xenografts following treatment with either vehicle (veh) or 12.5 mg/kg CX-
 784 3543 for 19 days. Tumor weights of TS543-sh590 (c) xenografts at study endpoint (See
 785 Materials and Methods) following treatment with either vehicle control (Veh) or 12.5
 786 mg/kg CX-3543 are also shown.

shCon-1	ATCTCGCTTGGGCGAGAGTAAG
shATRX-1	GGAAGCTAGCTCTTCAGAAA
shCon-2	CAACAAGATGAAGAGCACCAA
shATRX-2	GGAAAGATGATAAAGGAAA
shCon-3	CAACAAGATGAAGAGCACCAA
sh590	CGACAGAACTAACCCCTGTAA

Table 1: sequences of shRNA against ATRX

Tel 1/2 - Tel 1	GGTTTTGAGGGTGAGGGTGAGGGTGAGGGTGAGGGT
Tel 1/2 - Tel 2	TCCCGACTATCCCTATCCCTATCCCTATCCCTATCCCTA
Tel 2-F	CAAGTTTAAGGTTGTGTTTGTAC
Tel 2-R	AAATGAGTTGCAACAGGTACAAT
Tel X-F	TGTCTGGGTCTTTGGAGAGG
Tel X-R	CCTAACCCATCTGCTGGTTC
GAPDH CHIP-F	CGGGATTGTCTGCCCTAATTAT
GAPDH CHIP-R	GCACGGAAGGTCACGATGT
Myc-F	AGGGCTTCTCAGAGGCTTG
Myc-R	GCTGGAATTACTACAGCGAGTT
ZNF618-F	CGACGCCACCTAGAGGATAC
ZNF618-R	AATCTCTTACCCCTCCACTGC
ESR1-F	GCAGATCCAAGCTGTCTTTACTCA
ESR1-R	GGTGGGCAGAAGAAATCCTTT

Table 2: primer sequences of G4-ChIP-qPCR